

# An Adeno-Associated Viral Vector Capable of Penetrating the Mucus Barrier to Inhaled Gene Therapy

Gregg A. Duncan,<sup>1,2,10,11</sup> Namho Kim,<sup>1,3,11</sup> Yanerys Colon-Cortes,<sup>4</sup> Jason Rodriguez,<sup>1,2</sup> Marina Mazur,<sup>5</sup> Susan E. Birket,<sup>5</sup> Steven M. Rowe,<sup>5</sup> Natalie E. West,<sup>6</sup> Alessandra Livraghi-Butrico,<sup>7</sup> Richard C. Boucher,<sup>7</sup> Justin Hanes,<sup>1,2,3,8</sup> George Aslanidi,<sup>4,9</sup> and Jung Soo Suk<sup>1,2</sup>

<sup>1</sup>Center for Nanomedicine, Wilmer Eye Institute, Johns Hopkins University School of Medicine, Baltimore, MD 21231, USA; <sup>2</sup>Department of Ophthalmology, Johns Hopkins University School of Medicine, Baltimore, MD 21231, USA; <sup>3</sup>Department of Chemical and Biomolecular Engineering, Johns Hopkins University, Baltimore, MD 21218, USA; <sup>4</sup>Department of Pediatrics, University of Florida, Gainesville, FL 32610, USA; <sup>5</sup>Department of Medicine, Cystic Fibrosis Research Center, University of Alabama at Birmingham, Birmingham, AL 35294, USA; <sup>6</sup>Department of Medicine, Division of Pulmonary and Critical Care Medicine, Johns Hopkins University School of Medicine, Baltimore, MD 21287, USA; <sup>7</sup>Marsico Lung Institute/Cystic Fibrosis Research Center, The University of North Carolina at Chapel Hill School of Medicine, Chapel Hill, NC 27599, USA; <sup>8</sup>Departments of Biomedical Engineering, Environmental and Health Sciences, Oncology, Neurosurgery, and Pharmacology and Molecular Sciences, Johns Hopkins University, Baltimore, MD 21287, USA; <sup>9</sup>The Hormel Institute, University of Minnesota, Austin, MN 55912, USA; <sup>10</sup>Fischell Department of Bioengineering, University of Maryland, College Park, MD 20742, USA

**Diffusion of the viral vectors evaluated in inhaled gene therapy clinical trials to date are largely hindered within airway mucus, which limits their access to, and transduction of, the underlying airway epithelium prior to clearance from the lung. Here, we discovered that adeno-associated virus (AAV) serotype 6 was able to rapidly diffuse through mucus collected from cystic fibrosis (CF) patients, unlike previously tested AAV serotypes. A point mutation of the AAV6 capsid suggests a potential mechanism by which AAV6 avoids adhesion to the mucus mesh. Significantly greater transgene expression was achieved with AAV6 compared to a mucoadhesive serotype, AAV1, in air-liquid interface cultures of human CF bronchial epithelium with naturally secreted mucus or induced mucus hypersecretion. In addition, AAV6 achieved superior distribution and overall level of transgene expression compared to AAV1 in the airways and whole lungs, respectively, of transgenic mice with airway mucus obstruction. Our findings motivate further evaluation and clinical development of AAV6 for inhaled gene therapy.**

## INTRODUCTION

Past clinical trials testing viral gene vectors, including adenovirus (AdV) and adeno-associated virus (AAV) serotype 2, for inhaled gene therapy have failed to provide clinically significant benefits. These disappointing outcomes have been attributed to inefficient gene transfer to airway epithelium and generation of therapy-inactivating host immune responses.<sup>1</sup> Accordingly, recent advances in viral vector engineering have focused on enhancing the transduction of airway epithelium<sup>2–10</sup> and reducing immunogenicity.<sup>11,12</sup> Whereas underappreciated in early clinical studies, airway mucus has been recently recognized as another critical biological barrier to inhaled therapeutics.<sup>13–21</sup> The airway epithelium is protected by a secreted

mucus gel layer that traps most inhaled foreign materials, including gene vectors, and facilitates their removal from the airways via mucus clearance mechanisms.<sup>13,22,23</sup> In previous studies, we found that many clinically tested and commonly used viral vectors, including AdV, AAV1, AAV2, and AAV5, bind adhesively to human airway mucus,<sup>24,25</sup> impeding access to the epithelium that is required for successful transduction.

Recent studies comparing AAV serotypes for inhaled application revealed that AAV6 provided superior gene transfer efficacy *in vitro* and *in vivo* to other serotypes.<sup>2,26–28</sup> However, the underlying mechanisms are not fully understood, with one report suggesting a potential role of its ability to escape the proteasome degradation pathway.<sup>26</sup> In addition, many prior studies have been conducted using *in vitro* and *in vivo* models that lack the lung pathophysiology similar to that of patients with muco-obstructive lung diseases, such as cystic fibrosis (CF), chronic obstructive pulmonary disease (COPD), and asthma. To this end, we sought to evaluate the performance of AAV6 in the lung using physiologically relevant experimental conditions, including human CF sputum, a mucus-covered air-liquid interface (ALI) culture of human CF airway epithelium, and an advanced transgenic mouse model closely mimicking the lung environment found in muco-obstructive lung diseases. Using multiple particle tracking (MPT), we first investigated whether AAV6 was capable of avoiding entrapment within

Received 22 February 2018; accepted 19 March 2018;  
<https://doi.org/10.1016/j.omtm.2018.03.006>.

<sup>11</sup>These authors contributed equally to this work.

**Correspondence:** Jung Soo Suk, PhD, Center for Nanomedicine at the Wilmer Eye Institute, Johns Hopkins University School of Medicine, 400 N. Broadway, Robert H. and Clarice Smith Building, 6029, Baltimore, MD 21231, USA.

**E-mail:** [jsuk@jhmi.edu](mailto:jsuk@jhmi.edu)



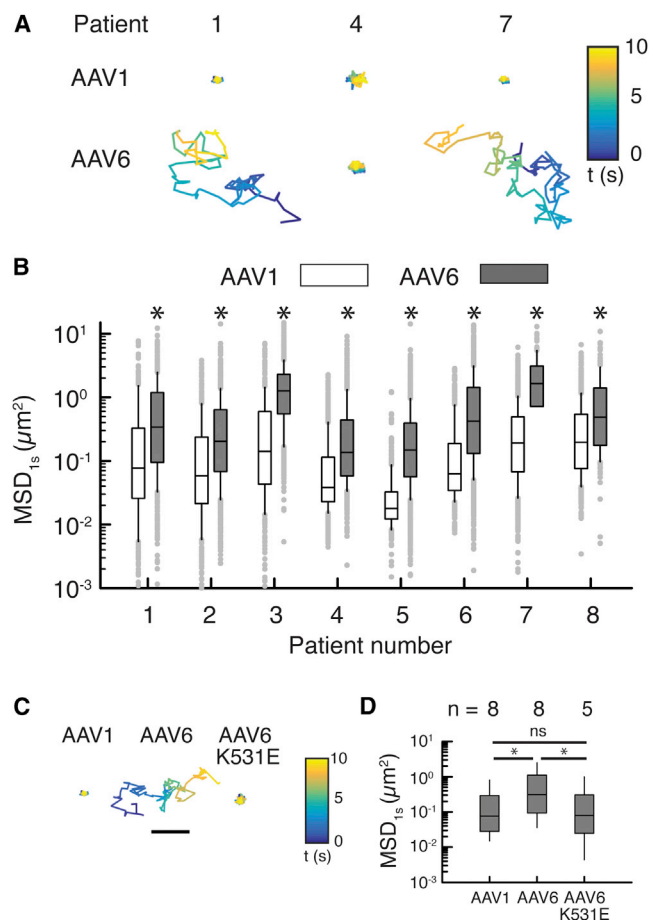


**Figure 1. AAV Diffusion in Spontaneously Expectored CF Sputum**

(A) Representative trajectories of AAV1 and AAV6 in sputum samples from 3 CF patients. Trajectories show 10 s of AAV motions. Color bar indicates the time ( $t$ ) of the trajectory in seconds. The scale bar represents 1  $\mu\text{m}$ . (B) Box-and-whisker plots of  $\text{MSD}_{1\text{s}}$  of AAV1 and AAV6 in sputum samples collected from 8 individual CF patients are shown. Maximum whisker length is 1.5 times the interquartile range; outliers are shown as dots. (C) Representative trajectories of AAV1, AAV6, and AAV6-K531E in CF sputum are shown. Trajectories show 10 s of AAV motions. Color bar indicates the time ( $t$ ) of the trajectory in seconds. The scale bar represents 1  $\mu\text{m}$ . (D) Box-and-whisker plots of  $\text{MSD}_{1\text{s}}$  for AAV1, AAV6, and AAV6-K531E in all patient samples tested are shown. Outliers are not shown. \* $p < 0.05$ ; Mann-Whitney test.

the mucus meshwork of CF sputum, unlike previously tested AAV serotypes.<sup>24,25</sup> We then determined the impact of the airway mucus barrier on the ability of AAV6 to mediate transgene expression in airway epithelium *in vitro* and *in vivo* and compared AAV6 to AAV1, a serotype shown to outperform the clinically tested AAV2<sup>29,30</sup> but unable to efficiently penetrate human CF sputum.<sup>25</sup>

## RESULTS

### AAV Diffusion in Freshly Collected CF Sputum

To assess the abilities of different AAV vectors to penetrate human airway mucus, we measured using MPT the diffusion rates

of Alexa Fluor 647 (AF647)-labeled AAV in freshly collected sputum samples spontaneously expectorated by CF patients. The percent solids content and mucin concentration of collected sputum samples were  $7.4 \pm 4.9\%$  and  $5.9 \pm 1.6 \text{ mg/mL}$ , respectively, in good agreement with previously reported values.<sup>31,32</sup> We have previously confirmed that our method of AF647 labeling does not significantly alter the natural surface property and transduction efficiency of AAV.<sup>25</sup> Consistent with our prior observation,<sup>25</sup> AAV1 displayed highly confined trajectories, indicating their entrapment within CF sputum. In contrast, AAV6 traveled far greater distances over time (Figure 1A). Quantitatively, AAV6 consistently exhibited greater diffusion rates, measured by mean squared displacement at a timescale of 1 s ( $\text{MSD}_{1\text{s}}$ ), compared to AAV1 in sputum samples collected from 8 different CF patients (Figure 1B).  $\text{MSD}_{1\text{s}}$  represents the average squared distance individual AAVs travel within a 1-s time interval and is directly proportional to their diffusion rates.<sup>33</sup> Based on the median of  $\text{MSD}_{1\text{s}}$ , AAV6 diffusion in CF sputum was enhanced by 3- to 10-fold in comparison to AAV1. Of note, we found that the diffusion rate of AAV6 was comparable to that of a synthetic gene delivery nanoparticle previously confirmed to efficiently penetrate CF sputum<sup>19</sup> (Figure S1). In order to further explore the differences in diffusion behaviors of AAV1 and AAV6 in CF sputum, we measured the diffusion rate of an AAV6 mutant, AAV6-K531E, which has been previously shown to confer AAV6 with an AAV1-like binding affinity to glycans.<sup>34</sup> The diffusion rates of AAV6-K531E in 5 different CF sputum samples were significantly lower than those of wild-type AAV6 and comparable to those of wild-type AAV1 (Figures 1C and 1D). We found that diffusion rates of AAV1 and AAV6 did not significantly correlate with solids content (i.e., percent dry weight) of sputum samples ( $R^2 = 0.05$ ), consistent with our prior observation with AAV2.<sup>25</sup>

### Impact of Apical Mucus on *In Vitro* AAV Transduction

Based on the significantly enhanced diffusion rates of AAV6 compared to AAV1 in CF sputum (Figure 1), we next sought to determine the impact of secreted mucus on the abilities of different AAV vectors to penetrate to the underlying airway epithelial cells and mediate transgene expression *in vitro*. We first examined *in vitro* transduction efficiency of AAV1, AAV6, and AAV6-K531E packaged with self-complementary EGFP gene (scAAV-EGFP) in human CF bronchial epithelial immortalized (CFBE41o<sup>-</sup>) cells, derived from a F508del homozygous CF patient, grown at an ALI where cells are differentiated into a mucus-secreting lung airway epithelium. Once fully differentiated, AAV-mediated GFP transgene expression was evaluated 2 weeks post-infection using confocal microscopy (Figures 2A–2C). We found that AAV6-treated CFBE41o<sup>-</sup> cultures exhibited  $\sim 2$ -fold greater coverage, defined as the total reporter-positive area divided by the total cell-covered surface area, and overall level of GFP transgene expression compared to AAV1-treated cultures, whereas both the coverage, and overall level were comparable between AAV6-K531E- and AAV1-treated cultures (Figures 2D and 2E). We then repeated the experiment using CFBE41o<sup>-</sup> ALI cultures treated to

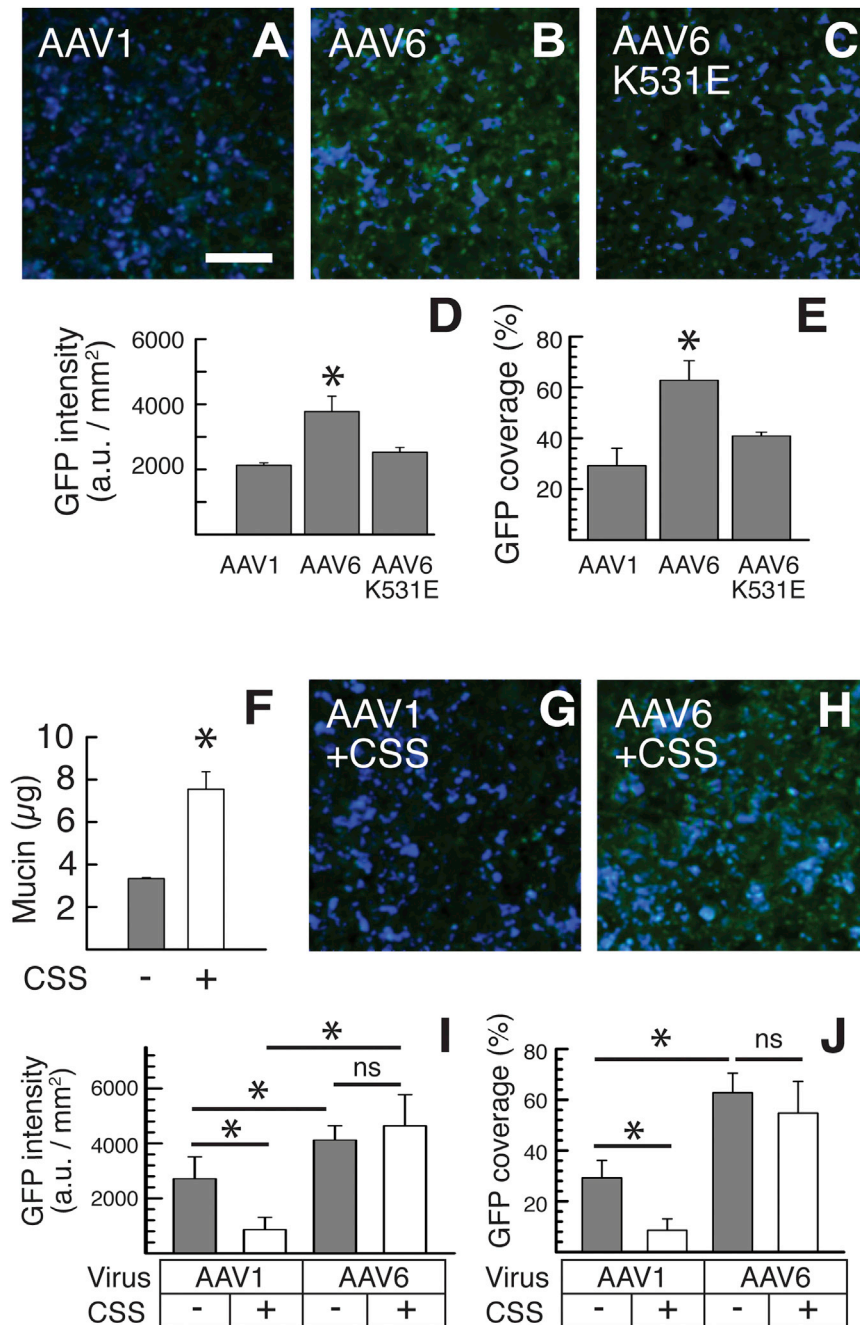


**Figure 2. In Vitro Transgene Expression in Human CFBE41o<sup>-</sup> ALI Cultures**

(A–C) Representative images of CFBE41o<sup>-</sup> ALI cultures transduced with (A) AAV1, (B) AAV6, and (C) AAV6-K531E. The scale bar represents 50 µm. (D and E) Image-based quantification of AAV-mediated GFP transgene expression in terms of (D) overall level and (E) relative coverage in CFBE41o<sup>-</sup> ALI cultures (n = 6) is shown. (F) Mucin contents of CFBE41o<sup>-</sup> ALI cultures before and after CSS treatment are shown. (G and H) Representative images of CFBE41o<sup>-</sup> ALI cultures transduced with (G) AAV1 and (H) AAV6 where cultures were pretreated overnight with CSS are shown. (I and J) Image-based quantification of AAV-mediated GFP transgene expression in terms of (I) overall level and (J) relative coverage in CSS-pretreated CFBE41o<sup>-</sup> ALI cultures (n = 6) is shown. \*p < 0.05; Student's t test (F) or one-way ANOVA (D, E, I, and J).

mucin level was ~3-fold greater in CSS-treated cultures than in untreated control cultures (Figure 2E). Subsequently, we compared the transduction efficiency of apically administered AAV1 and AAV6 in CSS-treated versus untreated CFBE41o<sup>-</sup> cultures. The AAV1-mediated coverage and overall level of GFP transgene expression were significantly reduced in CSS-treated CFBE41o<sup>-</sup> cultures compared to untreated cultures, whereas AAV6 retained those readouts regardless of the CSS-induced mucus hypersecretion (Figures 2F–2J).

To further test the effect of secreted mucus on AAV transduction, we evaluated AAV transduction in primary CF human bronchial epithelial (HBE) cells harvested from F508del homozygous CF patients, grown at an ALI with or without the removal of apically secreted mucus. We found that, whereas the coverage and overall level of GFP transgene expression mediated by AAV1 was significantly enhanced by washing the apical mucus with PBS, mucus removal did not affect the readouts when treated with AAV6 (Figure 3). Of note, the removal of apically secreted mucus

induce mucus hypersecretion. Mucus hypersecretion was established by incubating the cultures overnight with CF sputum supernatant (CSS) solution rich in pro-inflammatory cytokines, such as interleukin-1β (IL-1β), neutrophil elastase, and tumor necrosis factor α (TNF-α),<sup>35</sup> which has been previously shown to induce mucus hypersecretion in human airway epithelial ALI cultures.<sup>36</sup> Mucus hypersecretion was confirmed by measuring the quantity of mucin collected from the apical surfaces of CFBE41o<sup>-</sup> cultures where the

restored AAV1-mediated transduction to levels comparable to AAV6 (Figure 3).

#### **In Vivo AAV Transduction in a Mouse Model of Muco-obstructive Lung Disease**

To determine whether the mucus-penetrating property of AAV6 led to enhanced *in vivo* lung gene transfer, we compared the transduction efficiencies of AAV1 and AAV6 following

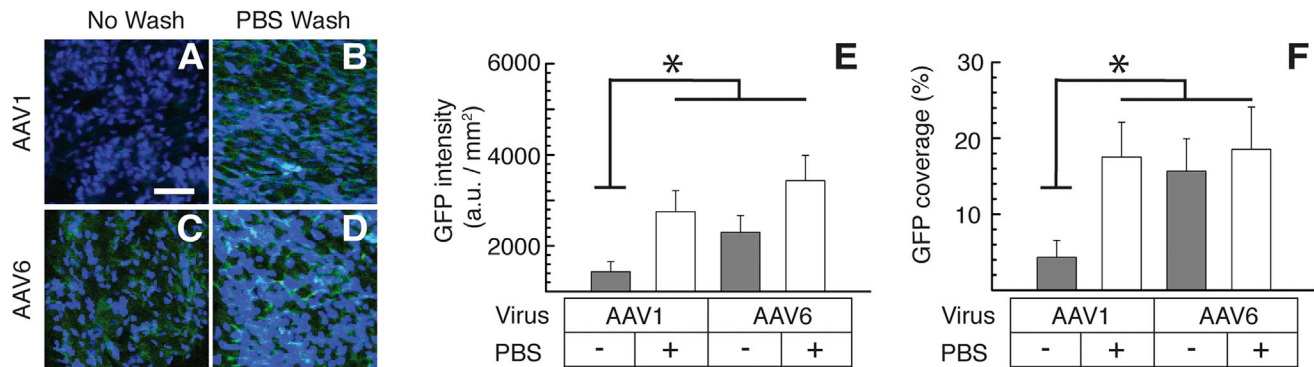


**Figure 3. *In Vitro* Transgene Expression in Primary CF HBE ALI Cultures**

(A–D) Representative images of GFP expression in primary CF HBE ALI cultures 2 weeks post-AAV transduction. Prior to the treatment, cultures were either left unwashed (no wash) or washed by PBS for the removal of the apically secreted mucus layer (PBS wash). The following conditions are shown: AAV1-treated HBE culture either unwashed (A) or washed (B) with PBS and AAV6-treated HBE culture either unwashed (C) or washed (D) with PBS. The scale bar represents 50  $\mu$ m. (E and F) Image-based quantification of AAV-mediated GFP transgene expression in terms of (E) overall level and (F) relative coverage in primary CF HBE ALI cultures with (+) or without (–) PBS wash ( $n = 3$ ) is shown. \* $p < 0.05$ ; one-way ANOVA.

administration via an aerosol-generating microsyringe to the lungs of *Scnn1b*-Tg mice overexpressing the  $\beta$ -subunit of the epithelial sodium channel ( $\beta$ ENaC) in the airways. *Scnn1b*-Tg mice spontaneously develop disease symptoms reminiscent of muco-obstructive lung diseases, such as mucus hyperconcentration/plugging, chronic airway inflammation, and airspace enlargement.<sup>37,38</sup> We confirmed the presence of mucus plugs in the airways of *Scnn1b*-Tg mice via immunohistochemistry, which was also distinguished through luminal DAPI staining of immune cells and DNA found within mucus plugs (Figure S2). For *in vivo* transduction studies,  $2 \times 10^{10}$  AAV1 or AAV6 packaged with single-stranded firefly luciferase-YFP fusion gene (ssAAV-Fluc-YFP) in 50  $\mu$ L PBS was administered into the lungs of *Scnn1b*-Tg mice.

The lung distribution of YFP transgene expression was visualized 2 weeks post-infection with AAV1 or AAV6, as shown in the representative confocal micrographs of proximal and distal airways (Figures 4A–4H). The relative coverage of YFP transgene expression in the airway and airspace was quantitatively assessed using a custom-written MATLAB software. In analyzing different, randomly selected regions of the airways and airspace, we observed a significantly greater YFP coverage in the mucus-covered/plugged airways (Figure S2A) of *Scnn1b*-Tg mice that intratracheally received AAV6 (28%), compared to the mice that received dose-matched AAV1 (13%; Figures 4B, 4D, and 4I). There was no significant difference in YFP coverage following the treatment with AAV6 (5%) and AAV1 (3%) in the airspace devoid of mucus secretion (Figures 4I and S2B). We also determined the luciferase activity of the whole-lung homogenates, an indicator of overall level of reporter transgene expression, from AAV1- and AAV6-treated *Scnn1b*-Tg mice, which revealed an  $\sim$ 2-fold greater bioluminescence intensity in the lungs of AAV6- versus AAV1-treated *Scnn1b*-Tg mice (Figure 4J).

## DISCUSSION

We have discovered that AAV6 is capable of efficiently diffusing through human CF sputum (i.e., mucus), which presents a critical extracellular barrier to effective inhaled gene therapy. *In vitro* studies in transformed and primary CF airway epithelial ALI cultures revealed that AAV6 gene transfer efficacy was not affected either by the presence of an endogenously secreted mucus layer or by induced mucus hypersecretion. In contrast, AAV1 transduction was markedly inhibited by both steady-state or induced mucus, presumably as a result of its inability to penetrate this barrier. The mucus-penetrating property of AAV6 was further confirmed *in vivo*. Inhaled AAV6 provided widespread and high-level transgene expression in the mucus-covered/plugged airways and the whole lungs, respectively, of a mouse model with airway mucus obstruction. This result agrees with our prior observations using synthetic mucus-penetrating drug and gene delivery nanoparticles that, unlike conventional mucoadhesive particles, exhibited widespread distribution and/or transgene expression in mouse lungs.<sup>14,17–19,39</sup> Importantly, the inhaled AAV6 mediated roughly 30% airway coverage of transgene expression, which is comparable to the percentage of human CF airway epithelial cells with cystic fibrosis transmembrane conductance regulator (CFTR) transgene expression ( $\sim$ 25%) that was previously shown to be sufficient to restore normal mucus transport rates *in vitro*.<sup>40</sup> Overall, efficient mucus penetration is likely a crucial mechanism by which AAV6 may achieve therapeutically relevant lung gene transfer.

In contrast to our observations, mucin was previously shown not to inhibit AAV1 transduction *in vitro*.<sup>34</sup> The discrepancy is likely due to the markedly lower mucin concentrations employed in this earlier study ( $\leq 0.5$  mg/mL),<sup>41</sup> which is about an order of magnitude or more lower than the concentrations in naturally or pathologically secreted airway mucus collected from human subjects or ALI cultures of primary CF HBE cells.<sup>31,42–45</sup> It should be noted that, unlike an

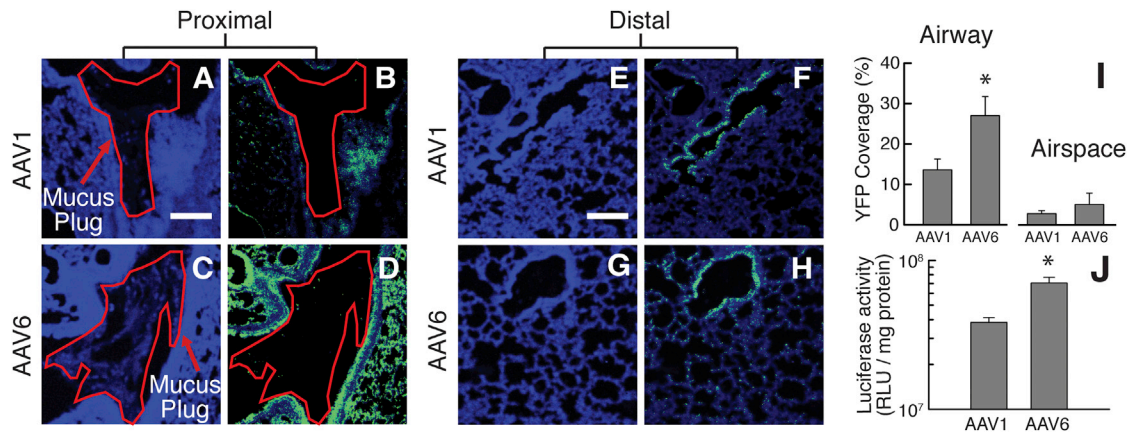


**Figure 4. In Vivo Transgene Expression in the Lungs of *Scnn1b*-Tg Mice following Intratracheal Administration of AAV1 or AAV6**

(A–H) Representative images of YFP expression (green) in the proximal (A–D) and distal airways/airspace (E–H). Confocal images of the proximal lung tissues from AAV1-treated mice showing cell nuclei only (A) or with YFP transgene expression (B) and from AAV6-treated mice showing cell nuclei only (C) or with YFP transgene expression (D). Confocal images of the distal lung tissues from AAV1-treated mice showing cell nuclei only (F) or with YFP transgene expression (G) and from AAV6-treated mice showing cell nuclei only (G) or with YFP transgene expression (H). Cell nuclei are stained with DAPI (blue). Regions of the airway lumen where mucus plugs were observed are outlined in red. The scale bar represents 200  $\mu\text{m}$ . (I) Image-based quantification of YFP expression coverage is shown ( $n = 3$  mice with 3 or 4 lung sections per mouse). (J) Luciferase expression mediated by AAV1 or AAV6 quantified for whole-lung homogenates is shown ( $n = 6$  mice). \* $p < 0.05$ ; Student's *t* test.

aqueous mucin solution, a mucus gel can trap nano-sized objects, such as AAV, via multivalent adhesive interactions as well as steric obstruction.<sup>14,16</sup> We also showed that, out of the 6 different capsid residues between AAV1 and AAV6, a single-amino-acid K-to-E substitution at the 531 position of the AAV6 capsid caused the mutant AAV6 (i.e., AAV6-K531E) to behave like AAV1,<sup>34</sup> a finding confirmed in airway mucus *in vitro* and *ex vivo*. We have previously demonstrated that heparan sulfate (HS) binding may be at least partially responsible for the adhesion of AAV2 to CF sputum.<sup>25</sup> However, it is unlikely the case here, as it has been shown previously that AAV6 binds to HS, whereas AAV1 and AAV6-K531E do not.<sup>34,46</sup> These findings suggest that glycan-mediated entrapment mechanisms may vary among AAV serotypes. In future studies, we aim to further explore the nature of interactions between different AAV serotypes and the glycans present on airway mucins.

The results of this study demonstrate the importance of using preclinical models that mimic key pathophysiological conditions of patients affected with muco-obstructive lung diseases in evaluating the efficacy of inhaled gene therapy. *Ex vivo* and *in vitro* experiments were designed to evaluate the ability of AAV6 to overcome pathological human airway mucus (i.e., CF sputum) and subsequently achieve efficient transduction of human airway epithelium. Past studies comparing the gene transfer efficacy of different AAV serotypes in human ALI cultures may have been affected by the large volumes (50–200  $\mu\text{L}$ )<sup>2,3,47–49</sup> applied on the apical surface during AAV administration, which dilute and potentially alter the barrier properties of apically secreted mucus. We thus used a small volume (i.e., 5  $\mu\text{L}$ ) in our experiments to minimize this issue. Most preclinical *in vivo* studies have also been conducted using healthy animals lacking critical pathological features in the lung.<sup>16</sup> In contrast, we evaluated the *in vivo* gene transfer efficacies of AAV serotypes possessing

different abilities to penetrate the airway mucus barrier using an established animal model of CF and COPD characterized by airway mucus plugging.

Future studies should address the persistence of transgene expression as well as the ability to readminister AAV without concern of therapy-inactivating immunogenicity. Toward this end, development and/or identification of a library of AAV vectors that possess the mucus-penetrating property while retaining high-level transduction efficiency would allow for serial vector administration for life-long therapeutic effects. In summary, we have demonstrated that the ability of AAV6 to penetrate the mucus barrier is a critical mechanism by which it achieves robust gene transfer to the lung airways. Our results underscore the importance of vectors used in inhaled gene therapy to overcome the mucus barrier, which is particularly reinforced in patients with muco-obstructive lung diseases.

## MATERIALS AND METHODS

### Production of Recombinant AAV Gene Vectors and Fluorescent Labeling

Recombinant AAV1, AAV6, and an AAV6 mutant, AAV6-K531E vectors were packaged with either self-complementary EGFP (scAAV-EGFP) or single-stranded firefly luciferase-YFP fusion (ssAAV-Fluc-YFP) gene as described previously.<sup>50,51</sup> Both reporter transgenes are expressed under the control of the ubiquitous chicken  $\beta$ -actin promoter (CBA). To engineer AAV6-K531E, a two-step PCR with reading-proof Turbo Pfu Polymerase (Stratagene) was used on plasmid pACGr2/c6 to introduce a single mutation;<sup>34,52</sup> primers were designed to make a change in an amino acid coding triplet from lysine (K; codon: AAG) to glutamic acid (E; codon: GAG) at 531 position of AAV capsid. The titers of DNase-I-resistant vector particles were determined by qPCR using the primer pair specific

for the CBA promoter, F-5'-TCCCATAGTAACGCCAATAGG-3' and R-5'-CTTGCCATATGATACACTTGATG-3', and SYBR GreenER PCR Master Mix (Invitrogen). Of note, two separate batches of AAV vectors were constructed and used for *in vitro* and *in vivo* transduction studies to ensure reproducibility. For visualization and tracking of individual viruses, AAV was labeled with the amine-reactive fluorescent dye, Alexa Fluor 647 carboxylic acid succinimidyl ester (AF647; Life Technologies), as previously described.<sup>25</sup> AF647-labeled AAVs were stored at  $-80^{\circ}\text{C}$  and thawed on ice prior to use.

### Formulation of Synthetic Mucus-Penetrating Gene Delivery Nanoparticles

For comparison with AAV diffusion in CF sputum, synthetic mucus-penetrating gene delivery nanoparticles were formulated as described previously.<sup>19</sup> Briefly, 5 kDa methoxy polyethylene glycol (PEG) N-hydroxysuccinimide (Sigma-Aldrich) was conjugated to 25 kDa branched polyethylenimine (PEI) (Sigma-Aldrich) to yield PEG<sub>5k</sub>-PEI copolymer. Nanoparticles were formed by the dropwise addition of 9 or 10 volumes of 0.2 mg/mL GFP-encoding plasmid DNA controlled by the cytomegalovirus promoter (Clontech) to 1 volume of a swirling polymer solution containing 25% unmodified PEI and 75% PEG<sub>5k</sub>-PEI copolymer, at an optimized nitrogen to phosphate ratio of 6. Twenty percent of the plasmid DNA used to assemble nanoparticles was fluorescently labeled by Cy3 dye using the Mirus Label IT Tracker Intracellular Nucleic Acid Localization Kit (Mirus Bio).

### CF Sputum Sample Collection and Biochemical Assay

CF sputum samples were collected under written informed consent, in accordance with the Johns Hopkins Institutional Review Board (IRB). Spontaneously expectorated sputum samples were collected from patients visiting the Adult Cystic Fibrosis Center at Johns Hopkins University. Particle-tracking experiments were conducted using samples stored at  $4^{\circ}\text{C}$  immediately after collection for up to 24 hr, based on our prior confirmation that the barrier properties of freshly collected sputum are maintained in this condition.<sup>14,31</sup> To reduce the effects of salivary contamination, any sample with a visible quantity of saliva was excluded. Patients involved in this study received no mucolytics other than Pulmozyme (i.e., dornase alfa) and/or hypertonic saline as part of their standard treatment regimen. Further information on the demographics of patients included in the study can be found in the supplement.

The percent solids content and mucin concentration of sputum samples were determined using previously reported methods.<sup>31</sup> For solids content, sputum samples were frozen in liquid N<sub>2</sub> and placed in a lyophilizer (FreeZone 4.5 Plus; Labconco) for at least 12 hr to completely extract water within individual samples. The percent solids content is defined as the ratio of mucus mass before and after the lyophilization. Mucin concentration was determined based on the reaction between 2-cyanoacetamide (Sigma-Aldrich) with O-linked glycoproteins (i.e., mucin) followed by a fluorometric assay, as previously described.<sup>31</sup>

### Multiple Particle Tracking in CF Sputum

The motions of AAV or synthetic mucus-penetrating gene delivery nanoparticles in sputum were tracked by fluorescent video microscopy and quantified by MPT analysis using a software custom-written in MATLAB (MathWorks), as previously reported.<sup>25,33</sup>

### In Vitro Transduction

The CFBE41o<sup>-</sup> cell line<sup>53</sup> (a gift from Drs. Cebotaru and Guggino from Johns Hopkins University) and primary CF human bronchial epithelial cells expressing the F508del mutant CFTR (CF HBE) were used for *in vitro* transduction studies. The University of Alabama at Birmingham IRB approved the use of primary cells. CFBE41o<sup>-</sup> cells were grown in minimum essential media with 10% fetal bovine serum, L-glutamine, penicillin/streptomycin, and puromycin (5  $\mu\text{g}/\text{mL}$ ). Primary CF HBE cells were expanded using co-culture with irradiated fibroblasts (R&D Systems) and conditional reprogramming via media containing a rho-associated protein kinase inhibitor.<sup>54,55</sup> CFBE41o<sup>-</sup> or primary CF HBE cells were grown in 0.33 cm<sup>2</sup> polyester membrane transwell inserts (Corning) at an ALI for 4–6 weeks until terminally differentiated. Once the ALI was established, CFBE41o<sup>-</sup> or primary CF HBE cells were maintained in the above-described growth media or PneumaCult-ALI Maintenance Medium (STEMCELL Technologies), respectively. A 5- $\mu\text{L}$  suspension of  $2 \times 10^9$  AAV vector genomes, either AAV1, AAV6, or AAV6-K531E, packaged with a gene encoding EGFP (i.e., scAAV-EGFP) was administered to the apical surface of the fully differentiated ALI cultures at a MOI of 5,000 to evaluate *in vitro* transduction efficiency. After an overnight incubation with AAV, 100  $\mu\text{L}$  of PBS was added to the apical chamber of inoculated cultures, incubated for 30 min at  $37^{\circ}\text{C}$ , and subsequently washed via aspiration.

We adapted a previously reported protocol to induce mucus hypersecretion in CFBE41o<sup>-</sup> ALI cultures.<sup>36</sup> Briefly, 5  $\mu\text{L}$  of CSS was added to both the apical and basolateral compartments and incubated overnight. The CSS solution was prepared by high-speed centrifugation (21,000  $\times g$ ) for 1 hr of 2.5 mL sputum pooled from 5 CF patients, followed by filtration through a 0.2- $\mu\text{m}$  ELF spin-filter (Molecular Probes). Apical mucin content of CFBE41o<sup>-</sup> ALI cultures was fluorometrically determined by the identical method used for the analysis of CF sputum. To remove apically secreted mucus from primary CF HBE ALI cultures, the apical chamber was incubated with 100  $\mu\text{L}$  of PBS at  $37^{\circ}\text{C}$  for 30 min, followed by removal via aspiration. GFP transgene expression was imaged using a confocal LSM 510 microscope (Zeiss) at 10 $\times$  and 20 $\times$  magnification and quantified using a custom-written software in MATLAB. To avoid artifacts presented by differences in focus between images, we used automated focusing (available in Zeiss Zen software) of DAPI nuclear staining and captured all images at this focal plane. Six or more randomly selected image fields were taken of each insert and used for quantification. The percentage of GFP coverage was defined as the GFP-positive area divided by the total cell-covered surface area, and the total GFP intensity was quantified as the average of total pixel intensity units for each dataset. Prior to quantitative analysis, all images were normalized by fluorescence of untreated control ALI cultures to eliminate the contribution of autofluorescence.

### In Vivo Transduction

All animals were treated in accordance with the policies and guidelines of the Johns Hopkins University Animal Care and Use Committee. Four-week old, congenic C57BL/6N transgenic mice with airway-specific overexpression of the epithelial sodium channel  $\beta$ -subunit ( $\beta$ ENaC, gene *Scnn1b*; i.e., *Scnn1b*-Tg mice)<sup>37</sup> were used for *in vivo* transduction studies. To evaluate the distribution and overall level of transgene expression in the lungs of *Scnn1b*-Tg mice, a 50- $\mu$ L solution of  $2 \times 10^{10}$  AAV packaged with a gene encoding luciferase-YFP fusion protein (i.e., ssAAV-Fluc-YFP) was delivered intratracheally using a microsyringe (MicroSprayer Aerosolizer Model IA-1C; Penn-Century; n = 3 and 6 mice per group for assessing the distribution and overall level of transduction, respectively). Animals were sacrificed 2 weeks post-administration to determine the distribution of YFP transgene expression in airways/airspace as well as luciferase activity of whole lung homogenates, a measure of overall transgene expression level. For the distribution study, lungs were harvested, flash-frozen in optimum cutting temperature (OCT) compound, and cryosectioned using a CM1950 cryostat (Leica Biosystems). Slides were immunologically stained using a AF488-conjugated GFP monoclonal antibody (Santa Cruz Biotechnology) and DAPI and subsequently imaged using a confocal LSM 510 microscope under 10 $\times$  and 20 $\times$  magnification. Four or more randomly selected image fields were taken from 3 lung tissue sections showing regions of the airways and airspace (i.e., total of at least 12 images per animal) for quantifying the distribution of transgene expression. To quantitatively assess the coverage of YFP transgene expression in airways/airspace, custom software written in MATLAB was used where images were blinded and airway regions were manually determined based on DAPI staining. The boundaries of airway and non-airway regions (i.e., anywhere outside of selected airway regions) were further refined using automated image thresholding. Percentage of YFP coverage was defined as the YFP-positive airway or airspace area divided by the total area of a respective compartment. Prior to quantitative analysis, all images were normalized by fluorescence of untreated *Scnn1b*-Tg lung tissue to eliminate the contribution of autofluorescence. To directly visualize mucus plugs in the airways of *Scnn1b*-Tg mice, slides were immunologically stained with anti-MUC5B (Santa Cruz Biotechnology; 5B#19-2E:sc-21768) and anti-MUC5AC (Thermo Fisher; MA5-12178) antibodies. For fluorescent tagging of MUC5AC and MUC5B, a biotinylated anti-mouse immunoglobulin G (IgG) (Sigma-Aldrich) was used as a secondary antibody, followed by a staining with ExtrAvidin-Cy3 (Sigma-Aldrich). Luciferase activity on lung tissue homogenates was measured using a standard luciferase assay kit (Thermo Fisher Scientific) and a 20/20n luminometer (Turner Biosystems).<sup>17,19</sup> The relative light intensity was normalized by total protein concentration measured by a standard bicinchoninic acid assay (Thermo Fisher Scientific).

### Statistical Analysis

Data were analyzed with statistical tests, including Student's t test using SigmaPlot 10.0 and a non-parametric Mann Whitney test using MATLAB R2014b. Multiple comparisons were performed by one-

way ANOVA using MATLAB R2014b. Data were considered statistically significant when  $p < 0.05$ . The statistical tests used in each dataset are indicated in the figure legends.

### SUPPLEMENTAL INFORMATION

Supplemental Information includes two figures and one table and can be found with this article online at <https://doi.org/10.1016/j.omtm.2018.03.006>.

### AUTHOR CONTRIBUTIONS

G.A.D., N.K., Y.C.-C., J.H., G.A., and J.S.S. constructed/characterized gene vectors and designed experiments. G.A.D., N.K., Y.C.-C., and J.R. performed experiments. N.E.W. obtained patient consent and collected patient samples. M.M., S.E.B., and S.M.R. prepared and provided primary human cystic fibrosis bronchial epithelial cells. A.L.-B. and R.C.B. provided the *Scnn1b*-Tg mouse model and relevant technical support. G.A.D., N.K., Y.C.-C., J.H., G.A., and J.S.S. wrote the manuscript. All authors read and approved the manuscript.

### CONFLICTS OF INTEREST

The mucus-penetrating particle technology described in this publication was developed at the Johns Hopkins University and is licensed to Kala Pharmaceuticals. J.H. is a founder of Kala Pharmaceuticals and currently serves as a consultant. J.H. and Johns Hopkins University own company stock; J.H.'s relationship with Kala Pharmaceuticals is subject to certain restrictions under university policy. The terms of this arrangement are being managed by the Johns Hopkins University in accordance with its conflict of interest policies.

### ACKNOWLEDGMENTS

We thank Liudmilla Ceboratu and William Guggino for providing the CFBE410<sup>+</sup> cells used in this work. This work was supported by the NIH (R01HL127413, R01HL136617, R35HL135816, P30DK072482, P30DK065988, and P30EY001765) and the Cystic Fibrosis Foundation (HANES16XX0, SUK1810, and R026-CR11).

### REFERENCES

- Griesenbach, U., and Alton, E.W.; UK Cystic Fibrosis Gene Therapy Consortium (2009). Gene transfer to the lung: Lessons learned from more than 2 decades of CF gene therapy. *Adv. Drug Deliv. Rev.* 61, 128–139.
- Limberis, M.P., Vandenberghe, L.H., Zhang, L., Pickles, R.J., and Wilson, J.M. (2009). Transduction efficiencies of novel AAV vectors in mouse airway epithelium *in vivo* and human ciliated airway epithelium *in vitro*. *Mol. Ther.* 17, 294–301.
- Yan, Z., Keiser, N.W., Song, Y., Deng, X., Cheng, F., Qiu, J., and Engelhardt. (2013). A novel chimeric adenoassociated virus 2/human bocavirus 1 parvovirus vector efficiently transduces human airway epithelia. *Mol. Ther.* 21, 2181–2194.
- Cooney, A.L., Abou Alaiwa, M.H., Shah, V.S., Bouzek, D.C., Stroik, M.R., Powers, L.S., Gansemer, N.D., Meyerholz, D.K., Welsh, M.J., Stoltz, D.A., et al. (2016). Lentiviral-mediated phenotypic correction of cystic fibrosis pigs. *JCI Insight* 1, e88730.
- Steines, B., Dickey, D.D., Bergen, J., Excoffon, K.J.D.A., Weinstein, J.R., Li, X., Yan, Z., Abou Alaiwa, M.H., Shah, V.S., Bouzek, D.C., et al. (2016). CFTR gene transfer with AAV improves early cystic fibrosis pig phenotypes. *JCI Insight* 1, e88728.
- Flotte, T.R., Fischer, A.C., Goetzmann, J., Mueller, C., Ceboaru, L., Yan, Z., Wang, L., Wilson, J.M., Guggino, W.B., and Engelhardt, J.F. (2010). Dual reporter comparative

- indexing of rAAV pseudotyped vectors in chimpanzee airway. *Mol. Ther* 18, 594–600.
7. Yan, Z., Feng, Z., Sun, X., Zhang, Y., Zou, W., Wang, Z., Jensen-Cody, C., Liang, B., Park, S.Y., Qiu, J., and Engelhardt, J.F. (2017). Human bocavirus type-1 capsid facilitates the transduction of ferret airways by adeno-associated virus genomes. *Hum. Gene Ther.* 28, 612–625.
  8. Griesenbach, U., Inoue, M., Meng, C., Farley, R., Chan, M., Newman, N.K., Brum, A., You, J., Kerton, A., Shoemark, A., et al. (2012). Assessment of F/HN-pseudotyped lentivirus as a clinically relevant vector for lung gene therapy. *Am. J. Respir. Crit. Care Med.* 186, 846–856.
  9. Alton, E.W., Beekman, J.M., Boyd, A.C., Brand, J., Carlon, M.S., Connolly, M.M., Chan, M., Conlon, S., Davidson, H.E., Davies, J.C., et al. (2017). Preparation for a first-in-man lentivirus trial in patients with cystic fibrosis. *Thorax* 72, 137–147.
  10. Excoffon, K.J., Koerber, J.T., Dickey, D.D., Murtha, M., Keshavjee, S., Kaspar, B.K., Zabner, J., and Schaffer, D.V. (2009). Directed evolution of adeno-associated virus to an infectious respiratory virus. *Proc. Natl. Acad. Sci. USA* 106, 3865–3870.
  11. Gernoux, G., Wilson, J.M., and Mueller, C. (2017). Regulatory and exhausted T cell responses to AAV capsid. *Hum. Gene Ther.* 28, 338–349.
  12. Tse, L.V., Klinc, K.A., Madigan, V.J., Castellanos Rivera, R.M., Wells, L.F., Havlik, L.P., Smith, J.K., Agbandje-McKenna, M., and Asokan, A. (2017). Structure-guided evolution of antigenically distinct adeno-associated virus variants for immune evasion. *Proc. Natl. Acad. Sci. USA* 114, E4812–E4821.
  13. Cone, R.A. (2009). Barrier properties of mucus. *Adv. Drug Deliv. Rev.* 61, 75–85.
  14. Duncan, G.A., Jung, J., Hanes, J., and Suk, J.S. (2016). The mucus barrier to inhaled gene therapy. *Mol. Ther.* 24, 2043–2053.
  15. Ferrari, S., Geddes, D.M., and Alton, E.W. (2002). Barriers to and new approaches for gene therapy and gene delivery in cystic fibrosis. *Adv. Drug Deliv. Rev.* 54, 1373–1393.
  16. Kim, N., Duncan, G.A., Hanes, J., and Suk, J.S. (2016). Barriers to inhaled gene therapy of obstructive lung diseases: A review. *J. Control. Release* 240, 465–488.
  17. Mastorakos, P., da Silva, A.L., Chisholm, J., Song, E., Choi, W.K., Boyle, M.P., Morales, M.M., Hanes, J., and Suk, J.S. (2015). Highly compacted biodegradable DNA nanoparticles capable of overcoming the mucus barrier for inhaled lung gene therapy. *Proc. Natl. Acad. Sci. USA* 112, 8720–8725.
  18. Schneider, C.S., Xu, Q., Boylan, N.J., Chisholm, J., Tang, B.C., Schuster, B.S., Henning, A., Ensign, L.M., Lee, E., Adstamgongkonkul, P., et al. (2017). Nanoparticles that do not adhere to mucus provide uniform and long-lasting drug delivery to airways following inhalation. *Sci. Adv.* 3, e1601556.
  19. Suk, J.S., Kim, A.J., Trehan, K., Schneider, C.S., Cebotaru, L., Woodward, O.M., Boylan, N.J., Boyle, M.P., Lai, S.K., Guggino, W.B., and Hanes, J. (2014). Lung gene therapy with highly compacted DNA nanoparticles that overcome the mucus barrier. *J. Control. Release* 178, 8–17.
  20. Suk, J.S. (2016). Could recent advances in DNA-loaded nanoparticles lead to effective inhaled gene therapies? *Nanomedicine (Lond.)* 11, 193–196.
  21. Forier, K., Messiaen, A.S., Raemdonck, K., Deschout, H., Rejman, J., De Baets, F., Nelis, H., De Smedt, S.C., Demeester, J., Coenye, T., and Braeckmans, K. (2013). Transport of nanoparticles in cystic fibrosis sputum and bacterial biofilms by single-particle tracking microscopy. *Nanomedicine (Lond.)* 8, 935–949.
  22. Fahy, J.V., and Dickey, B.F. (2010). Airway mucus function and dysfunction. *N. Engl. J. Med.* 363, 2233–2247.
  23. Knowles, M.R., and Boucher, R.C. (2002). Mucus clearance as a primary innate defense mechanism for mammalian airways. *J. Clin. Invest.* 109, 571–577.
  24. Hida, K., Lai, S.K., Suk, J.S., Won, S.Y., Boyle, M.P., and Hanes, J. (2011). Common gene therapy viral vectors do not efficiently penetrate sputum from cystic fibrosis patients. *PLoS ONE* 6, e19919.
  25. Schuster, B.S., Kim, A.J., Kays, J.C., Kanzawa, M.M., Guggino, W.B., Boyle, M.P., Rowe, S.M., Muzyczka, N., Suk, J.S., and Hanes, J. (2014). Overcoming the cystic fibrosis sputum barrier to leading adeno-associated virus gene therapy vectors. *Mol. Ther.* 22, 1484–1493.
  26. Li, W., Zhang, L., Wu, Z., Pickles, R.J., and Samulski, R.J. (2011). AAV-6 mediated efficient transduction of mouse lower airways. *Virology* 417, 327–333.
  27. Kurosaki, F., Uchibori, R., Mato, N., Sehara, Y., Saga, Y., Urabe, M., Mizukami, H., Sugiyama, Y., and Kume, A. (2017). Optimization of adeno-associated virus vector-mediated gene transfer to the respiratory tract. *Gene Ther.* 24, 290–297.
  28. McClain, L.E., Davey, M.G., Zoltick, P.W., Limberis, M.P., Flake, A.W., and Peranteau, W.H. (2016). Vector serotype screening for use in ovine perinatal lung gene therapy. *J. Pediatr. Surg.* 51, 879–884.
  29. Liu, X., Luo, M., Trygg, C., Yan, Z., Lei-Butters, D.C., Smith, C.I., Fischer, A.C., Munson, K., Guggino, W.B., Bunnell, B.A., and Engelhardt, J.F. (2007). Biological differences in rAAV transduction of airway epithelia in humans and in old world non-human primates. *Mol. Ther.* 15, 2114–2123.
  30. Liu, X., Luo, M., Guo, C., Yan, Z., Wang, Y., and Engelhardt, J.F. (2007). Comparative biology of rAAV transduction in ferret, pig and human airway epithelia. *Gene Ther.* 14, 1543–1548.
  31. Duncan, G.A., Jung, J., Joseph, A., Thaxton, A.L., West, N.E., Boyle, M.P., Hanes, J., and Suk, J.S. (2016). Microstructural alterations of sputum in cystic fibrosis lung disease. *JCI Insight* 1, e88198.
  32. Henderson, A.G., Ehre, C., Button, B., Abdullah, L.H., Cai, L.H., Leigh, M.W., DeMaria, G.C., Matsui, H., Donaldson, S.H., Davis, C.W., et al. (2014). Cystic fibrosis airway secretions exhibit mucin hyperconcentration and increased osmotic pressure. *J. Clin. Invest.* 124, 3047–3060.
  33. Schuster, B.S., Ensign, L.M., Allan, D.B., Suk, J.S., and Hanes, J. (2015). Particle tracking in drug and gene delivery research: state-of-the-art applications and methods. *Adv. Drug Deliv. Rev.* 91, 70–91.
  34. Wu, Z., Asokan, A., Grieger, J.C., Govindasamy, L., Agbandje-McKenna, M., and Samulski, R.J. (2006). Single amino acid changes can influence titer, heparin binding, and tissue tropism in different adeno-associated virus serotypes. *J. Virol.* 80, 11393–11397.
  35. Sagel, S.D., Chmiel, J.F., and Konstan, M.W. (2007). Sputum biomarkers of inflammation in cystic fibrosis lung disease. *Proc. Am. Thorac. Soc.* 4, 406–417.
  36. Ribeiro, C.M.P., Hurd, H., Wu, Y., Martino, M.E., Jones, L., Brighton, B., Boucher, R.C., and O’Neal, W.K. (2009). Azithromycin treatment alters gene expression in inflammatory, lipid metabolism, and cell cycle pathways in well-differentiated human airway epithelia. *PLoS ONE* 4, e5806.
  37. Mall, M., Grubb, B.R., Harkema, J.R., O’Neal, W.K., and Boucher, R.C. (2004). Increased airway epithelial Na<sup>+</sup> absorption produces cystic fibrosis-like lung disease in mice. *Nat. Med.* 10, 487–493.
  38. Mall, M.A., Harkema, J.R., Trojanek, J.B., Treis, D., Livraghi, A., Schubert, S., Zhou, Z., Kreda, S.M., Tilley, S.L., Hudson, E.J., et al. (2008). Development of chronic bronchitis and emphysema in beta-epithelial Na<sup>+</sup> channel-overexpressing mice. *Am. J. Respir. Crit. Care Med.* 177, 730–742.
  39. Huang, X., Chisholm, J., Zhuang, J., Xiao, Y., Duncan, G., Chen, X., Suk, J.S., and Hanes, J. (2017). Protein nanocages that penetrate airway mucus and tumor tissue. *Proc. Natl. Acad. Sci. USA* 114, E6595–E6602.
  40. Zhang, L., Button, B., Gabriel, S.E., Burkett, S., Yan, Y., Skiadopoulos, M.H., Dang, Y.L., Vogel, L.N., McKay, T., Mengos, A., et al. (2009). CFTR delivery to 25% of surface epithelial cells restores normal rates of mucus transport to human cystic fibrosis airway epithelium. *PLoS Biol.* 7, e1000155.
  41. Wu, Z., Miller, E., Agbandje-McKenna, M., and Samulski, R.J. (2006).  $\alpha$ 2,3 and  $\alpha$ 2,6 N-linked sialic acids facilitate efficient binding and transduction by adeno-associated virus types 1 and 6. *J. Virol.* 80, 9093–9103.
  42. Sanders, N.N., De Smedt, S.C., Van Rompaey, E., Simoens, P., De Baets, F., and Demeester, J. (2000). Cystic fibrosis sputum: a barrier to the transport of nanoparticles. *Am. J. Respir. Crit. Care Med.* 162, 1905–1911.
  43. Suk, J.S., Boylan, N.J., Trehan, K., Tang, B.C., Schneider, C.S., Lin, J.M., Boyle, M.P., Zeitlin, P.L., Lai, S.K., Cooper, M.J., and Hanes, J. (2011). N-acetylcysteine enhances cystic fibrosis sputum penetration and airway gene transfer by highly compacted DNA nanoparticles. *Mol. Ther.* 19, 1981–1989.
  44. Schuster, B.S., Suk, J.S., Woodworth, G.F., and Hanes, J. (2013). Nanoparticle diffusion in respiratory mucus from humans without lung disease. *Biomaterials* 34, 3439–3446.



45. Kesimer, M., Ford, A.A., Ceppe, A., Radicioni, G., Cao, R., Davis, C.W., Doerschuk, C.M., Alexis, N.E., Anderson, W.H., Henderson, A.G., et al. (2017). Airway mucin concentration as a marker of chronic bronchitis. *N. Engl. J. Med.* 377, 911–922.
46. Xie, Q., Lerch, T.F., Meyer, N.L., and Chapman, M.S. (2011). Structure-function analysis of receptor-binding in adeno-associated virus serotype 6 (AAV-6). *Virology* 420, 10–19.
47. Bals, R., Xiao, W., Sang, N., Weiner, D.J., Meegalla, R.L., and Wilson, J.M. (1999). Transduction of well-differentiated airway epithelium by recombinant adeno-associated virus is limited by vector entry. *J. Virol.* 73, 6085–6088.
48. Yan, Z., Zak, R., Zhang, Y., Ding, W., Godwin, S., Munson, K., Peluso, R., and Engelhardt, J.F. (2004). Distinct classes of proteasome-modulating agents cooperatively augment recombinant adeno-associated virus type 2 and type 5-mediated transduction from the apical surfaces of human airway epithelia. *J. Virol.* 78, 2863–2874.
49. Mitomo, K., Griesenbach, U., Inoue, M., Somerton, L., Meng, C., Akiba, E., Tabata, T., Ueda, Y., Frankel, G.M., Farley, R., et al. (2010). Toward gene therapy for cystic fibrosis using a lentivirus pseudotyped with Sendai virus envelopes. *Mol. Ther.* 18, 1173–1182.
50. Aslanidi, G.V., Rivers, A.E., Ortiz, L., Song, L., Ling, C., Govindasamy, L., Van Vliet, K., Tan, M., Agbandje-McKenna, M., and Srivastava, A. (2013). Optimization of the capsid of recombinant adeno-associated virus 2 (AAV2) vectors: the final threshold? *PLoS ONE* 8, e59142.
51. Pandya, J., Ortiz, L., Ling, C., Rivers, A.E., and Aslanidi, G. (2014). Rationally designed capsid and transgene cassette of AAV6 vectors for dendritic cell-based cancer immunotherapy. *Immunol. Cell Biol.* 92, 116–123.
52. Sayroo, R., Nolasco, D., Yin, Z., Colon-Cortes, Y., Pandya, M., Ling, C., and Aslanidi, G. (2016). Development of novel AAV serotype 6 based vectors with selective tropism for human cancer cells. *Gene Ther.* 23, 18–25.
53. Cozens, A.L.A., Yezzi, M.J., Chin, L., Simon, E.M., Finkbeiner, W.E., Wagner, J.A., and Gruenert, D.C. (1992). Characterization of immortal cystic fibrosis tracheobronchial gland epithelial cells. *Proc. Natl. Acad. Sci. USA* 89, 5171–5175.
54. Horani, A., Nath, A., Wasserman, M.G., Huang, T., and Brody, S.L. (2013). Rho-associated protein kinase inhibition enhances airway epithelial Basal-cell proliferation and lentivirus transduction. *Am. J. Respir. Cell Mol. Biol.* 49, 341–347.
55. Suprynowicz, F.A., Upadhyay, G., Krawczyk, E., Kramer, S.C., Hebert, J.D., Liu, X., Yuan, H., Cheluvraj, C., Clapp, P.W., Boucher, R.C., Jr., et al. (2012). Conditionally reprogrammed cells represent a stem-like state of adult epithelial cells. *Proc. Natl. Acad. Sci. USA* 109, 20035–20040.